J. Biochem. 122, 430-437 (1997)

A Novel Chloride-Binding Site Modulates the Heme-Copper Binuclear Center of the *Escherichia coli bo*-Type Ubiquinol Oxidase[1]

Tomoyasu Hirano,* Tatsushi Mogi,*,[2] Motonari Tsubaki,† Hiroshi Hori,‡ Yutaka Orii,§ and Yasuhiro Anraku*

*Department of Biological Sciences, Graduate School of Science, The University of Tokyo, Hongo, Bunkyo-ku, Tokyo 113; †Department of Life Science, Faculty of Science, Himeji Institute of Technology, Kamigoori-cho, Akou-gun, Hyogo 678-12; ‡Department of Biophysical Engineering, Faculty of Engineering Science, Osaka University, Toyanaka, Osaka 560; and §Department of Public Health, Graduate School of Medicine, Kyoto University, Kyoto 606

Received for publication, April 8, 1997

Cytochrome *bo*-type ubiquinol oxidase in *Escherichia coli* belongs to a superfamily of the heme-copper respiratory oxidases and catalyzes the redox-coupled proton pumping. Previous studies [Y. Orii, T. Mogi, M. Sato-Watanabe, T. Hirano, and Y. Anraku (1995) *Biochemistry* 34, 1127-1132] suggest that it requires chloride ions for the facilitated heme *b*-to-heme *o* intramolecular electron transfer. To extend our previous studies on chloride binding by *bo*-type ubiquinol oxidase, we prepared two kinds of chloride-bound enzymes, UQO-412 and UQO-409, and a chloride-depleted enzyme, UQO-407, and examined their spectroscopic and enzymatic properties. UQO-412, which exhibits the Soret peak at 412 nm in the air-oxidized state, was obtained by purification with anion-exchange liquid chromatography, and UQO-409 was derived from UQO-412 by extensive washing and showed a 3-nm blue shift. UQO-407 was obtained from UQO-409 by omitting chloride ions from buffers throughout purification and showed a further blue shift in the Soret peak and the pronounced chloride-sensitive EPR signals at $g=6$ and $g=3.15$, which are attributable to spin-spin exchange interaction at the binuclear center. Kinetic studies on chloride binding by UQO-407 revealed the presence of a chloride-binding site with a K_d value of 3.5 mM. Flow-flash experiments demonstrated that the heme *b*-to-heme *o* electron transfer was perturbed in both UQO-409 and UQO-407, although steady state enzyme activities of three UQOs were indistinguishable. The present studies demonstrated that the *E. coli bo*-type ubiquinol oxidase is endowed with a novel chloride-binding site which controls the electromagnetic state of the heme-copper binuclear center. Further, we suggest that the intramolecular electron transfer in the enzyme requires diffusible molecules other than the bound chloride ion.

Key words: chloride binding site, cytochrome *bo*, electron transfer, heme-copper binuclear center, terminal oxidase.

Cytochrome *bo*-type ubiquinol oxidase (UQO) of the aerobic respiratory chain in *Escherichia coli* functions as a predominant terminal oxidase under highly aerated growth conditions (*1*). It belongs to the heme-copper terminal oxidase superfamily (*2*) and catalyzes not only redox-coupled proton pumping but also scalar proteolytic reactions (*3*), the two-electron oxidation of ubiquinol-8 (Q_8H_2) at the periplasmic side and the four-electron reduction of molecular oxygen at the cytoplasmic side of the inner membrane.

Subunit I of UQO binds all the metal centers, low-spin heme *b*, high-spin heme *o*, and Cu_B (*4, 5*). The latter two centers are antiferromagnetically coupled in the air-oxidized state and form the heme-copper binuclear center (*6, 7*). Photoaffinity crosslinking studies using an azido-quinone derivative revealed that subunit II provides a binding site(s) for substrate (*8*). Besides a low-affinity quinol-oxidation site (Q_L), UQO has a high-affinity quinone-binding site (Q_H) which can stabilize a ubisemiquinone radical and appears to be essential for catalytic functions (*9-11*; Sato-Watanabe, M., Mogi, T., Anraku, Y., and Orii, Y., unpublished results). The bound Q_8 at the Q_H site seems to mediate electron transfer from the Q_L site to low-spin heme *b* and provides the fourth electron to complete a single turnover of dioxygen reduction, like Cu_A of cytochrome *c* oxidase (*12, 13*). Subsequently, a long range electron transfer from heme *b* to heme *o* takes place within subunit I, probably through a covalent bond system consisting of side-chains of heme ligands and their connecting

[1] This work was supported in part by Grants-in-Aid for Scientific Research on Priority Areas (08249106 and 08268216), for Scientific Research (A) (07558221) and (B) (08458202), and for Exploratory Research (08878097) from the Ministry of Education, Science, Sports and Culture of Japan. This is the paper XXVII in the series "Structure-function studies on the *E. coli* cytochrome *bo* complex."

[2] To whom correspondence should be addressed. Fax: +81-3-3812-4929

Abbreviations: UQO, *bo*-type ubiquinol oxidase; Q_nH_2, ubiquinol-*n*; Q_H, the high-affinity quinone-binding site; Q_L, the low-affinity quinol-oxidation site; Q_n, ubiquinone-*n*; HPLC, high performance liquid chromatography; SM, sucrose monolaurate; EPR, electron paramagnetic resonance.

peptide bonds "His[421]-Phe[420]-His[419]" (*4, 14*). Finally, dioxygen is reduced to water at the heme *o*-Cu_B binuclear center, where both preferential binding and reduction of dioxygen are promoted by Cu_B (*15*).

Time-resolved resonance Raman spectroscopy of UQO demonstrated the formation of the oxy intermediate, which then decays to the oxoferryl species, and thus suggests that the dioxygen reduction proceeds as found in mammalian cytochrome *c* oxidase (*16*). Flow-flash studies revealed that ligand binding is the rate-limiting step in the reaction of UQO with dioxygen, while intramolecular electron transfer is rate-limiting in that of mammalian cytochrome *c* oxidase (*12*). We noticed recently that the heme *b*-to-heme *o* intramolecular electron transfer in the chloride-depleted UQO was severely perturbed as compared to that of the chloride-bound UQO (*13*). The heme *b*-to-heme *o* electron transfer seems to require chloride ion(s) for maintaining a subtle molecular structure around the metal centers (*13*).

In this article we isolated two chloride-bound and one chloride-depleted enzyme preparations and extended our spectroscopic and enzymatic studies on chloride binding by the *E. coli* UQO. Based on these observations, we suggest that UQO contains a novel chloride-binding site which controls the electromagnetic state of the heme-copper binuclear center.

EXPERIMENTAL PROCEDURES

Purification of UQO—UQO was isolated from the cytochrome *bo*-overproducing strains GO103/pMFO2 (*cyo*$^+$ *Δcyd/cyo*$^+$; Ref. *7*) and GO103/pHN3795-1 (*cyo*$^+$*Δcyd/cyo*$^+$; Ref. *15*). The preparations are classified into three groups based on the purification procedures and their absorption maxima in the air-oxidized state. UQO-412 (*i.e.*, Cl-UQO in Ref. *13*) was isolated by DEAE-5PW HPLC using the Tris-HCl/NaCl buffer system containing 0.1% (w/v) sucrose monolaurate (SM; Mitsubishi-Kasei Food, Tokyo). UQO-409 was obtained from UQO-412 by washing with 50 mM Tris-HCl (pH 7.4) containing 0.1% SM with and then without 1 mM EDTA *via* ultrafiltration using Centriprep 100 (Millipore) (*7*). UQO-407 (*i.e.*, SO_4-UQO in Ref. *13*) was isolated by HPLC using the Tris-H_2SO_4/Na_2SO_4 buffer system containing 0.1% SM and was washed with 50 mM Tris-H_2SO_4 (pH 7.4) containing 0.1% SM with and then without 1 mM EDTA. UQO-407 can be also obtained by dialysis of UQO-409 as described below. Enzyme concentration was estimated from heme content as described previously (*7*).

Removal of Bound Chloride Ions from UQO by Dialysis—UQO-409 (*ca.* 0.5 mM) was diluted to 50 μM with 50 mM Tris-H_2SO_4 or Tricine-Tris (pH 7.4) containing 0.1% SM. Samples (*ca.* 1 ml) were dialyzed against 2 liters of 50 mM Tricine-Tris (pH 7.4) containing 0.1% SM for three days using a Spectrum dialysis tube (molecular weight cut-off of 50 kDa).

Enzyme Assay—Quinol oxidase activity was determined spectrophotometrically (*9*). Measurements were done in 50 mM Tris-HCl (pH 7.4) containing 0.1% SM (for UQO-412 and UQO-409) or 50 mM Tris-H_2SO_4 (pH 7.4) containing 0.1% SM (for UQO-407). The apparent K_m and V_{max} values were determined by double-reciprocal plots at the Q_1H_2 concentrations of 20, 25, 33, 50, and 200 μM.

Optical Spectroscopy—Absolute visible spectra of each preparation (2.5 μM) were recorded at room temperature with a Shimadzu UV-3000 double wavelength spectrophotometer (Shimadzu, Kyoto) (*17*). The air-oxidized (*i.e.*, as isolated) enzyme in the buffer used for enzyme assay was anaerobically reduced with 5 mM sodium dithionite in a rubber-capped cuvette, then a CO-bound form was prepared from the reduced enzyme by replacing N_2 atmosphere with CO. Low temperature spectra of the air-oxidized enzyme (10 μM) were taken at 77 K using an optical cell with a 2-mm light path, and the second-order finite difference spectra of the Soret peak were calculated with a $\Delta\lambda$ = 4.9 nm. Preincubation of UQO with 0.1 M NaCl was done on ice for one day. The reaction of fully reduced UQO (2 μM) with dioxygen was investigated by using a flow-flash technique on an apparatus described previously (*12, 13*). The response time of the detector for measurement of a time scale of 10 ms was 1 μs.

EPR Spectroscopy—EPR measurements with the air-oxidized enzyme (400 μM) were carried out at X-band (9.23 GHz) microwave frequency with a Varian E-12 EPR spectrometer with 100-kHz field modulation (*7*). An Oxford flow cryostat (ESR-900) was used at 5 K. Accuracy of the *g* values was ±0.01.

Kinetic Analysis of Chloride-Binding to UQO-407—Upon addition of NaCl, absorbance change of UQO-407 (2.5 μM) in 50 mM Tris-H_2SO_4 containing 0.1% SM was monitored with a Shimadzu UV-3000 double wavelength spectrophotometer in a dual beam mode. Initial rates of the absorbance decrease at 402.5 nm relative to that at 411 nm (*i.e.*, isosbestic point) were determined at room temperature. The apparent K_d value was determined by double-reciprocal plots at NaCl concentrations of 4, 5, 6.67, 10, 20, and 80 mM.

RESULTS

Visible Spectroscopic Analysis—Absolute spectra of UQO-412 [*i.e.*, Cl-UQO (*13*)], UQO-409 (*7, 9*), and UQO-407 [*i.e.*, SO_4-UQO (*13*)] were recorded under air-oxidized (as isolated), dithionite-reduced and reduced CO-bound conditions in the absence and presence of 0.1 M NaCl (Fig. 1 and Table I). Extensive washing of the Cl-bound UQO, UQO-412, *via* ultrafiltration resulted in a 3 nm blue-shift of the Soret peak in the air-oxidized state (UQO-412 and -409 in Fig. 1). Moreover, chloride-depletion from UQO-409 by washing or dialysis caused a further blue-shift of the Soret peak to 407 nm. In contrast, dialysis on UQO-412 resulted in only a slight change of the Soret peak (Table I). SDS-polyacrylamide gel electrophoresis analysis showed that relative amounts of subunits I, II, III, and IV were unaffected by these treatments (data not shown). This suggests that a loss of other diffusible factor(s) which controls the 412 nm-to-409 nm transition is a prerequisite for a further blue-shift. The 409-to-407 nm blue-shift can be reversed by incubation of UQO-407 with 0.1 M NaCl, while the Soret peak of UQO-409 and UQO-412 was unaffected by addition of NaCl (Fig. 1D and Table I). This indicates that a bound chloride ion(s) controls the Soret peak maximum of the air-oxidized UQO. This was confirmed by dialysis of UQO-409 against 50 mM Tricine-Tris buffer (pH 7.4) containing 0.1% SM. The resultant preparation showed the Soret peak at 407 nm, which was also shifted back to 409 nm upon addition of 0.1 M NaCl (Table

I). Subsequently, the molecular structure of the binuclear center of the air-oxidized UQOs was probed with cyanide, which forms a Fe_O(III)-CN-Cu_B(II) bridging structure (7). Overnight incubation of the air-oxidized UQOs with 1 mM KCN in all cases resulted in blue-shifts of the Soret peak to 414 nm (data not shown), indicating that there is no difference in the molecular environment at the binuclear center of the cyanide-bound UQOs.

In contrast to the air-oxidized enzymes, the Soret peak maxima of the dithionite-reduced forms and the CO-bound forms showed only slight differences (*i.e.*, the Soret peak at about 427 and 417 nm, respectively) (Table I). These observations are consistent with kinetic analysis of Q_1H_2 oxidase activity showing that differences in the Soret peak maxima did not affect the steady state oxidase activity (data not shown). All three preparations exhibited the same K_m value of 50 μM and the apparent V_{max} value of about 900 e·s^{-1}.

To resolve spectral components attributable to the blue shift of the Soret peak, second-order finite difference spectra of the air-oxidized UQOs at 77 K were calculated with $\Delta\lambda = 4.9$ nm (Fig. 2). UQO-409 showed three negative peaks at 402, 413, and 418 nm, and a loss of the bound chloride ion increased the 402-nm component (Fig. 2, A and C). The 413-nm component may be ascribed mainly to low-spin heme *b*, since this peak position is close to the Soret peak (415 nm) of the His419Ala mutant oxidase, where high-spin heme *o* was absent because of a lack of its proximal ligand (*18*). Overnight incubation of UQO-407 with 0.1 M NaCl reduced the intensity of the 402-nm component, consistent with the effect on the Soret peak shift (Fig. 1D). Similarly, the 402-nm component increased in UQO-409 which had been prepared by dialysis, and the blue sift was suppressed by addition of NaCl (data not shown). Thus, these results indicate that the 409 nm-to-407 nm blue-shift in the Soret peak of the air-oxidized UQO is attributable to changes in the molecular environment of high-spin heme *o* upon removal of a bound chloride ion(s).

Ion Specificity of the Chloride Binding Site—To examine the halide ion specificity of the novel chloride-binding site, we determined the Soret peak maximum of UQO after overnight incubation with 0.1 M sodium salts (Table II). The effects of NaCl and NaBr differed greatly from those of NaF and NaI, which caused blue-shifts of the Soret peak. We then recorded time-dependent spectral changes in UQO-407 to resolve spectral components in the Soret peak shifts (Fig. 3). Addition of NaCl or NaBr increased in intensities of both a trough at 402.5 nm and a peak at 418.5 nm, while NaF and NaI induced a blue-shift of the 413-nm component to 398 nm with a slight intensity change (Fig. 3). The 402.5-nm trough seems to be related to the 402-nm

TABLE I. **Visible spectroscopic properties of UQOs under various conditions.** Absolute UV-visible spectra of UQO-412 and UQO-409 in 50 mM Tris-HCl (pH 7.4) containing 0.1% SM, UQO-407 in 50 mM Tris-H_2SO_4 (pH 7.4) containing 0.1% SM before and after dialysis against 50 mM Tricine-Tris (pH 7.4) containing 0.1% SM were recorded at room temperature. The enzymes were used at 2.5 μM.

Preparation	Dialysis	Soret peak (nm)			
		Air-oxidized		Reduced	CO-bound
		None	+0.1 M NaCl		
UQO-412	–	412	412	428	417.5
	+	411	NT[a]	427	418
UQO-409	–	409	409	427	417
	+	407	409	427	417
UQO-407	–	407	409	427	417
	+	407	410	427	417

[a]Not tested.

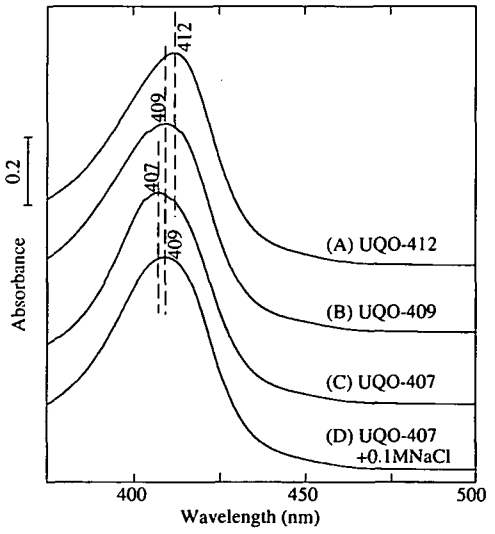

Fig. 1. **Absolute visible spectra of UQO-412 (A), UQO-409 (B), and UQO-407 (C, D) in the air-oxidized state.** UQOs were isolated from the cytochrome *bo*-overproducing strain GO103/pHN3795-1 (*cyo*$^+$*Δcyd*/*cyo*$^+$). Absolute spectra of 2.5 μM enzyme in 50 mM Tris-HCl (pH 7.4) containing 0.1% SM (A, B) or in 50 mM Tris-H_2SO_4 (pH 7.4) containing 0.1% SM (C, D) were recorded at room temperature in the absence (A-C) and presence of 0.1 M NaCl (D).

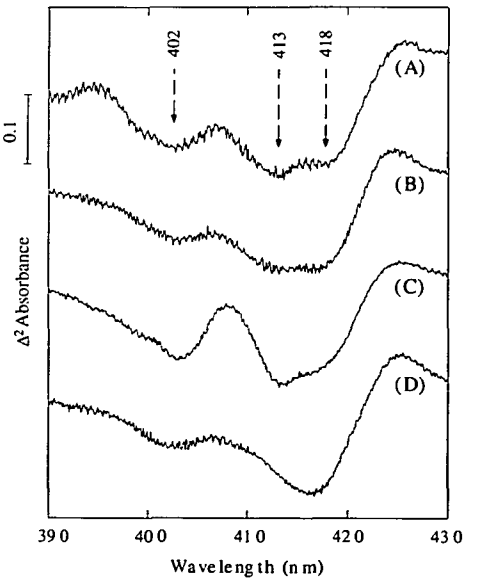

Fig. 2. **Second-order finite difference spectra of the air-oxidized UQO-409 (A, B) and UQO-407 (C, D) at 77 K in the absence (A, C) and presence (B, D) of 0.1 M NaCl.** Low temperature spectra of the air-oxidized enzymes (10 μM) were recorded at 77 K using an optical cell with a 2-mm light path and their second-order finite difference spectra were calculated with a $\Delta\lambda$ value of 4.9 nm. Other details are described in the legend to Fig. 1.

component in the second-order finite spectrum of UQO-407 at 77 K (Fig. 2). Binding of Cl or Br ions to UQO-407 increased the intensities of the α and β peaks, 550 and 525 nm, respectively, to similar amplitudes, and decreased slightly the intensities of the ferric high-spin marker band at 630 nm (*19, 20*) and the 660-nm band. The former peak, an indicator of its transition probability, is attributable to integral spin systems with zero field splitting terms comparable to the Zeeman interaction (*21, 22*). Fluoride binding increased the intensities of both bands and induced a small blue shift of the Soret peak, as reported previously (*19, 20, 23, 24*), while addition of NaI did not affect the absorption over 600 nm. These data suggest that UQO contains a novel chloride- and bromide-specific binding site, which controls the Soret peak of ferric high-spin heme *o* but is different from the site(s) for fluoride and iodide ions.

To determine a dissociation constant for the chloride binding by UQO-407, we measured initial rates for the chloride-induced absorbance change at the Soret region ($A_{402.5}-A_{411}$). Double reciprocal plot analysis was carried out at final concentrations of NaCl from 4 to 80 mM and yielded a linear correlation with a K_d value of 3.5 mM, confirming the presence of a specific chloride-binding site(s) in UQO (Fig. 4).

TABLE II. **Effect of sodium halides on the Soret peak of the air-oxidized UQOs.** The air-oxidized enzymes (2.5 μM for UQO-409 and UQO-407 or 1 μM for UQO-412) in 50 mM Tris-H_2SO_4 (pH 7.4) containing 0.1% SM were incubated with 50 mM NaCl, NaBr, NaF, or NaI at 4°C overnight and their absolute UV-visible spectra were recorded at room temperature.

Preparation	Soret peak (nm)				
	None	NaCl	NaBr	NaF	NaI
UQO-412	412	411.5	412	407	409
UQO-409	409	409	408.5	405	407.5
UQO-407	407	409	409	405	406

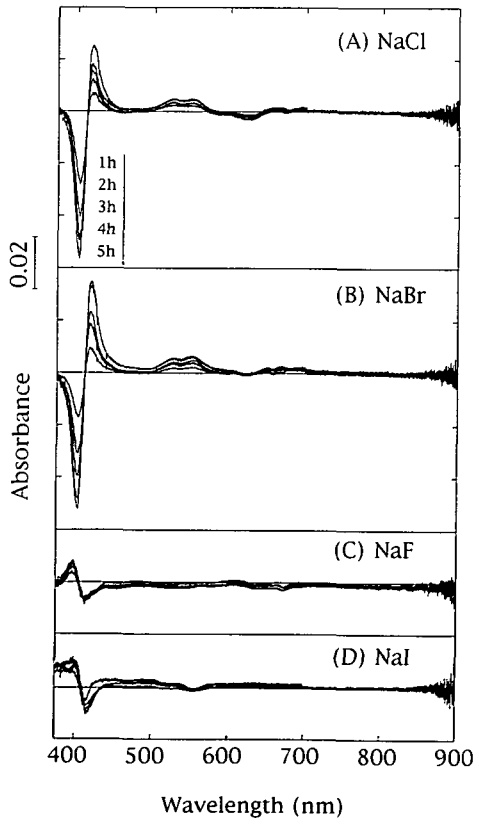

Fig. 3. **Time-dependence of difference spectra of the air-oxidized UQO-407 after addition of NaCl (A), NaBr (B), NaF (C), and NaI (D).** The spectra of the air-oxidized enzyme (5 μM) in 50 mM Tris-H_2SO_4 (pH 7.4) containing 0.1% SM and 0.1% skim milk were taken 1, 2, 3, 4, and 5 h after addition of sodium halides at a final concentration of 50 mM. The spectrum just after addition of each sodium halide was taken as a reference.

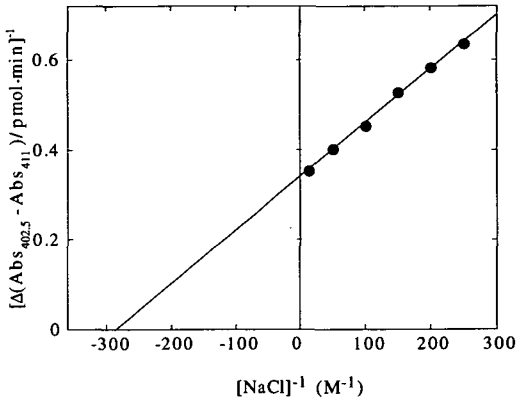

Fig. 4. **Double reciprocal plot analysis of chloride binding to the air-oxidized UQO-407.** Chloride binding to the air-oxidized enzyme (2.5 μM) in 50 mM Tris-H_2SO_4 (pH 7.4) containing 0.1% SM was initiated by addition of NaCl, and the rate of increase in the difference absorbance [$A_{402.5}-A_{411}$] was monitored at room temperature.

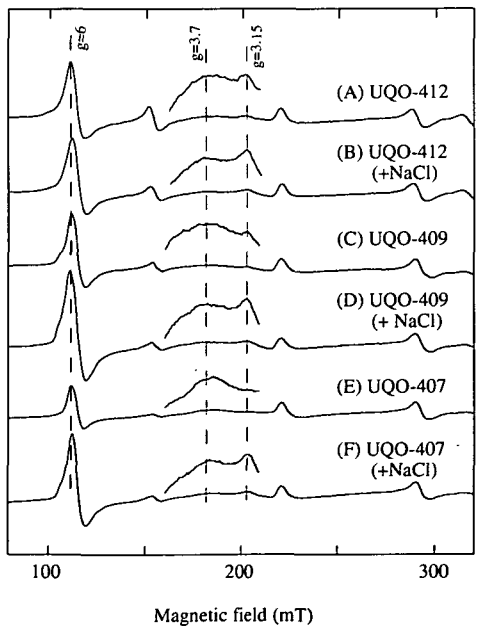

Fig. 5. **EPR spectra of the air-oxidized UQO-412 (A, B), UQO-409 (B, D), and UQO-407 (E, F) in the absence (A, C, E) and presence (B, D, F) of 0.1 M NaCl.** EPR measurements of the air-oxidized enzyme (0.4 mM) were carried out at 5 K and at X-band (9.23 GHz) microwave frequency with 100-kHz field modulation. Other experimental conditions were: modulation amplitude, 1 mT; microwave power, 5 mW.

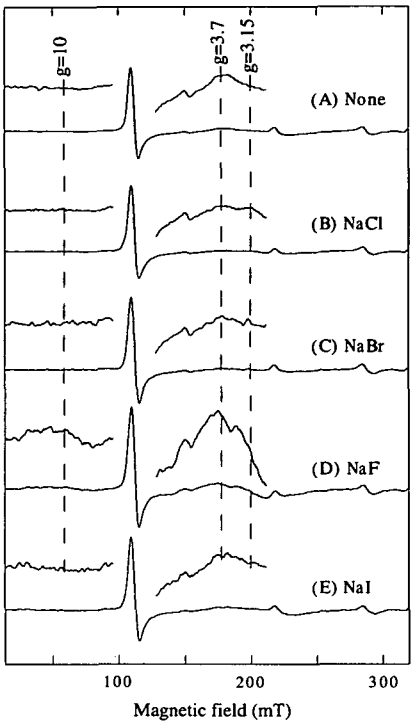

Fig. 6. **Effects of halide ions on the EPR signals of the chloride-depleted UQO, UQO-407, in the air-oxidized state.** UQO-407 (0.4 mM) as isolated (A) was incubated overnight on ice with 50 mM NaCl (B), NaBr (C), NaF (D), and NaI (E). EPR measurements were carried out at 5 K as described in the legend to Fig. 5.

EPR Spectroscopic Analysis—The heme-copper binuclear center of three UQO preparations was analyzed by EPR spectroscopy at 5 K (Fig. 5). In the air-oxidized state, UQO-412 exhibits a high-spin signal at $g=6$, low-spin signals at $g_z=2.98$ and $g_y=2.26$, and signals attributed to spin-spin exchange interactions at the binuclear center at $g=3.7$ and 3.15 (Fig. 5), as reported previously (*6, 7, 24*). The major part of the high-spin heme Fe^{3+} is strongly spin-spin coupled to Cu_B^{2+} center and therefore EPR-invisible (*6, 7, 18, 25, 26*). It should be noted that the $g=6$ signal of UQO-407 is only one-half of those of UQO-412 and UQO-409, indicating that the binuclear center of UQO-407 is more tightly spin-spin coupled upon removal of the bound chloride ion. Addition of 0.1 M NaCl to UQO-412 resulted in slight increase of the $g=3.15$ signal. In UQO-409 and UQO-407, both the $g=6$ and the $g=3.15$ signals increased significantly in intensity upon addition of NaCl (Fig. 5, D and F). Subsequently, the effects of other halide ions on the EPR signals were examined after incubation of the air-oxidized UQOs with 0.1 M sodium salts (Fig. 6). The effects of NaBr were similar to those of NaCl, as found in the visible spectroscopic analysis (Table II and Fig. 3). In contrast, the spin-decoupled $g=6$ signal was unaffected by fluoride or iodide ions, and the addition of NaF resulted in the formation of a species with a broad feature at $g=10$ and a series of features at near $g=3.2$, 3.8, and 4.7, as reported previously (*19, 23, 24*). These observations indicate that the effects of NaCl and NaBr are quite different from those of NaF and NaI.

Reaction of UQOs with Dioxygen—Dioxygen reduction kinetics of the three UQOs was examined by the flow-flash method (Fig. 7). An absorption change at 428 nm following reaction of the fully-reduced UQO-412 (Cl-UQO) with 145 μM dioxygen exhibited a single exponential decay (Fig. 7A), while both UQO-407 (SO_4-UQO) and UQO-409 showed a discrete biphasic decay (Fig. 7, B and C). The reaction of the fully reduced UQO-412 is almost completed within 1 ms, and the resultant species showed the α and Soret peaks at 562.4 and 414.5 nm, respectively, which were tentatively assigned to the pulsed form (*12*). In contrast, UQO-409 and -407 exhibited an intense α peak at 563 nm, attributable to the reduced low-spin heme *b*, and the broad Soret peaks from 420 to 415 nm, suggesting that the heme *b*-to-heme *o* electron transfer was perturbed in these preparations. Spectroscopic features of the resulting species and of the air-oxidized three UQO preparations are different from those of the oxoferryl species produced by reaction of the air-oxidized enzyme (*i.e.*, 406.5 nm) with hydrogen peroxide (*27*). This species is characterized by the Soret peak at 411 nm, increased absorbance at 555 nm, a weak feature at 624 nm, and disappearance of the broad $g=3.7$ signal (*27*). This and a previous observation (*13*) that the effect of chloride depletion from UQO on the dioxygen kinetics is irreversible suggest that the facilitated heme *b*-to-heme *o* intramolecular electron transfer requires an unidentified factor, which can be removed from UQO by either extensive washing or dialysis, other than the bound chloride ion.

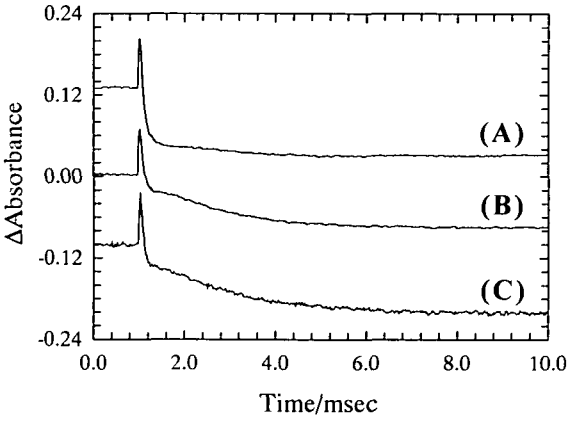

Fig. 7. **Time courses for reaction of the fully reduced UQO-412 (A), UQO-409 (B), and UQO-407 (C) with dioxygen followed at 428 nm.** UQOs in 50 mM Tris-HCl (pH 7.4) containing 0.1% SM (UQO-412 and UQO-409) or 50 mM Tris-H_2SO_4 (pH 7.4) containing 0.1% SM (UQO-407) were mixed with dioxygen at final concentrations of 2.5 and 145 μM, respectively, at 20°C. The traces are positioned with arbitrary offsets for clarity, and the abrupt absorption increase represents a release of the reduced enzyme upon photolysis of the CO adduct.

DISCUSSION

The *E. coli bo*-type ubiquinol oxidase has been extensively studied as a model system of the heme-copper terminal oxidases, since it is amenable to molecular biological studies. Structural models for the redox metal centers proposed on the basis of site-directed mutagenesis studies (Refs. *4, 5* for reviews) were confirmed by recent X-ray crystallographic studies on cytochrome *c* oxidase (*28, 29*). Possible pathways for proton translocation and electron

transfer (*4, 14, 18, 25, 28–31*) are now being subjected to experimental tests. To dissect electron transfer in UQO into elementary processes, it is essential to establish purification procedures for UQO that is characterized by a kinetically intact and homogeneous structure.

In contrast to the Soret peaks of the reduced form (427–428 nm) and the reduced CO-bound form (415–416 nm), the values reported for the air-oxidized UQO vary widely from 406.5 (*20, 27*) to 410±1 (*10, 19, 25, 32, 33*) nm. Differences in purification procedures (*e.g.*, detergents, *etc.*) might be a major cause for the variation in the Soret peak of the isolated UQO, and differences in heme composition (*31*) might also contribute. Preparations with the Soret peak at 406.5 (*20, 27*), 410 (*33*), and 411 (*19*) nm have been isolated from the cytochrome *bo*-overproducing strains, and the variability of heme O synthase activity might alter the heme composition. However, we found no difference in the heme B to heme O ratio (*ca.* 1 : 1) of purified UQOs isolated from a cytochrome *bd*-deficient strain harboring a multicopy expression vector (*15, 16*) or a single copy expression vector (*7, 10*). In addition, the variability of the Soret peak position cannot be attributed to the presence of the oxoferryl species in our preparation.

Recently, we have reported that the facilitated heme *b*-to-heme *o* intramolecular electron transfer exhibits a single component kinetics (*12*) and requires chloride ions (*13*). Since the effect of chloride ions was irreversible, we extended the previous study by isolating the Cl-bound and Cl-depleted UQOs, which show different Soret absorption maxima in the air-oxidized state. We examined the correlation of the Soret peak position with properties of the binuclear center and the dioxygen kinetics and found for the first time that the difference in the Soret peak maximum was associated with perturbations at the binuclear center and in the dioxygen kinetics. We demonstrated herein that UQO-412 can be transformed to UQO-409 and UQO-407 by a sequential loss of diffusible small molecules and the bound chloride ion, respectively. Since the bound phospholipids have been found in crystal structures for both bacterial and bovine cytochrome *c* oxidase (*28, 34*), phospholipids may play a functional role to maintain facilitated intramolecular electron transfer in UQO. Recently, Puustinen *et al.* (*35*) studied the kinetics of the dioxygen reaction of the fully reduced UQO and reported that binding of a single Q_8 molecule to UQO converts the reaction kinetics from monophasic to multiphasic kinetics. The product of monophasic reaction showed the α peak at 557 nm and the Soret peak at about 420 nm (*35*) and was assigned to the oxoferryl intermediate (*27*). However, we found that the UQO isolated from a ubiquinone biosynthesis mutant (*ΔubiA*) exhibited multiphasic kinetics (Sato-Watanabe *et al.*, unpublished results) and that incubation of UQO-412 and UQO purified in Triton X-100 with either Q_1 or Q_8 did not alter the reaction kinetics from monophasic to multiphasic (data not shown). The reaction product of UQO-412 with dioxygen exhibited the α peak at 564 nm and the Soret peak at 424 nm, which are different from those of the oxoferryl species produced by reaction with hydrogen peroxide (*27*) and of the fast reaction product of Puustinen *et al.* (*35*). Furthermore, the turnover number of UQO is about 900 $e \cdot s^{-1}$, indicating that the reduction of dioxygen can be completed within 4 ms. Thus, we assume that the bound Q_8 at the Q_H site of the fully reduced UQO can donate the fourth electron to complete the dioxygen reduction, thereby facilitating intramolecular electron transfer (*10, 11, 13*).

Localization and Role of the Chloride-Binding Site—The present study showed that removal of the bound chloride ion from UQO does not affect steady state enzyme activity and low-spin heme *b* but results in perturbation of spin-spin exchange interactions at the binuclear center in the air-oxidized state. Geier *et al.* (*36*) have reported that when yeast cytochrome *c* oxidase was isolated in the presence of chloride, more than 90% of the population showed the fast cyanide-binding kinetics. In the chloride-depleted enzyme, the fast form was reduced to 70%. Similar observations on the fast and slow forms of bovine cytochrome *c* oxidase have been attributed to chloride binding to the binuclear center (*37*). However, yeast preparations showed the same steady state activity and Soret peak (424 nm) in the air-oxidized state (*36*). Further, chloride depletion had a minor effect on the amplitude of the $g=6$ high-spin signal, and the fast-to-slow conversion was incomplete. Hence, the chloride-binding site in yeast cytochrome *c* oxidase must be similar to the one found in the present study on UQO.

Addition of NaCl to the Cl-depleted UQO caused a transition of ferric heme *o* from high-spin to low-spin state in the visible absorption spectra whereas the $g=6$ high-spin signal of ferric heme *o* increased in the EPR spectra. This discrepancy can be explained as follows. Due to antiferromagnetic spin-spin exchange coupling between Fe^{3+}, $S=5/2$, and Cu^{2+}, $S=1/2$, most of the $g=6$ signal of the air-oxidized UQO is invisible (*6, 7, 25*), as reported for mammalian cytochrome *c* oxidase (*38*). Removal of the bound chloride ion from UQO is likely to cause a subtle conformational change that increases the population in tightly spin-spin exchange coupled state, and thus decreases the intensity of the $g=6$ signal (see UQO-407 in Fig. 5). Rebinding of chloride ions to the Cl-depleted UQO is expected to restore the conformation and thus the spin-spin coupling at the binuclear center. Indeed, the $g=3.15$ signal attributable to another form of the more weakly spin-spin exchange coupled state regains its intensity upon addition of NaCl. Some population of the ferric heme *o* may be completely spin-spin decoupled and the $g=6$ high-spin EPR signal intensity, therefore, increased (Fig. 5). A minor population of the ferric heme *o* might be further converted to the low-spin state, which was detected in the visible absorption difference spectra (Fig. 3). These results indicate that the chloride-binding site is close to the binuclear center. Extended X-ray absorption fine structure studies on the air-oxidized bacterial quinol oxidases (*39, 40*) and mammalian cytochrome *c* oxidase (*41*) suggested the presence at the binuclear center of either sulfur or chloride, which may mediate spin-spin exchange as a bridging ligand. Since neither cysteine nor methionine is conserved at around the binuclear center of this oxidase superfamily (*2*), this atom, if present, is probably a bound chloride ion. Our observations, however, suggest that the bound chloride ion that modulates the binuclear center cannot be a bridging ligand. X-ray crystallographic studies on cytochrome *c* oxidase support the absence of a bridging ligand in the air-oxidized state (*28, 29*).

The chloride-binding site in human red and green color vision pigments is responsible for a large bathochromic

shift (1,132 cm^{-1}) of the retinal chromophore and has been identified as His^{197} and Lys^{200} in loop IV/V (*42*). Similarly, it is possible that the bound chloride ion in UQO modulates electromagnetically the heme-copper binuclear center through long range interactions and is crucial in maintaining a subtle molecular structure of the binuclear center. Since the intracellular concentration of chloride ions in *E. coli* is well above the K_d value of the chloride-binding site in cytochrome *bo* (*43*), this site seems physiologically important in regulation of the terminal oxidase. All the redox metal centers in subunit I of the heme-copper respiratory oxidases are located close to the periplasmic side (*4, 5, 17, 18, 28, 29*), therefore, the novel chloride-binding site is likely to be located at the periplasmic ends of putative transmembrane helices VI-VIII and X that hold the binuclear metal center. Conserved basic amino acid residues in the periplasmic loops (*e.g.*, Arg^{80} in loop I/II, Arg^{307}-Lys^{308} in loop VI/VII, and Arg^{481}-Arg^{482} in loop XI/XII) may serve as a binding site for chloride and bromide ions and/or anchors for the heme propionate groups. Furthermore, our spectroscopic studies clearly show that the binding site(s) for fluoride and iodide ions is different from the chloride/bromide-specific binding site. Fluoride may directly coordinate to ferric high-spin heme *o* or perturb spin-spin exchange interaction at the binuclear center through direct binding to Cu_B^{2+}.

In the present study, we demonstrated that UQO can be prepared in three distinct forms that show different spectroscopic and enzymatic properties. Among them, UQO-412 is the most suitable for kinetic studies on the reduction of dioxygen. The biphasic nature of the dioxygen reduction kinetics in UQO-409 and UQO-407 seems attributable to a loss of small molecules (*e.g.*, phospholipids) from the oxidase complex, because composition of subunits and the metal centers of the three UQOs were indistinguishable. Our data suggest that UQO is endowed with the novel chloride- (and bromide-) specific binding site which is close to the binuclear center though it is located at the surface of subunit I molecule. Spectroscopic studies indicate that the chloride-binding site is required for maintaining a subtle molecular environment of the binuclear center. To further understand the molecular mechanism which couples redox reactions with proton pumping, identifications of the chloride-binding site and the factor essential for the facilitated intramolecular electron transfer are now underway.

We thank R.B. Gennis (University of Illinois) for the *E. coli* strain GO103, M. Ohno (Eisai Co., Ltd., Tsukuba) for Q_1, and T. Tsuchiya (Okayama University) for discussion.

REFERENCES

1. Anraku, Y. and Gennis, R.B. (1987) The aerobic respiratory chain of *Escherichia coli*. *Trends Biochem. Sci.* **12**, 262-266
2. Saraste, M., Holm, L., Lemieux, L., Lübben, M., and van der Oost, J. (1991) The happy family of cytochrome oxidases. *Biochem. Soc. Trans.* **19**, 608-612
3. Puustinen, A., Finel, M., Haltia, T., Gennis, R.B., and Wikström, M. (1991) Properties of the two terminal oxidases of *Escherichia coli*. *Biochemistry* **30**, 3936-3942
4. Mogi, T., Nakamura, H., and Anraku, Y. (1994) Molecular structure of a heme-copper redox center of the *Escherichia coli* ubiquinol oxidase: Evidence and model. *J. Biochem.* **116**, 471-477
5. García-Horsman, J.A., Barquera, B., Rumbley, J, Ma, J., and Gennis, R.B. (1994) The superfamily of heme-copper respiratory oxidases. *J. Bacteriol.* **176**, 5587-5600
6. Salerno, J.C., Bolgiano, B., Poole, R.K., Gennis, R.B., and Ingledew, J.W. (1990) Heme-copper and heme-heme interactions in the cytochrome *bo*-containing quinol oxidase of *Escherichia coli*. *J. Biol. Chem.* **265**, 4364-4368
7. Tsubaki, M., Mogi, T., Anraku, Y., and Hori, H. (1993) Structure of heme-copper binuclear center of the cytochrome *bo* complex of *Escherichia coli*: EPR and Fourier-transform infrared spectroscopic studies. *Biochemistry* **32**, 6065-6072
8. Welter, R., Gu, L.-Q., Yu, L., Yu, C.-A., Rumbley, J., and Gennis, R.B. (1994) Identification of the ubiquinone-binding site in the cytochrome bo_3-ubiquinol oxidase of *Escherichia coli*. *J. Biol. Chem.* **269**, 28834-28838
9. Sato-Watanabe, M., Mogi, T., Miyoshi, H., Iwamura, H., Matsushita, K., Adachi, O., and Anraku, Y. (1994) Structure-function studies on the ubiquinol oxidation site of the cytochrome *bo* complex from *Escherichia coli* using *p*-benzoquinones and substituted phenols. *J. Biol. Chem.* **269**, 28899-28907
10. Sato-Watanabe, M., Mogi, T., Ogura, T., Kitagawa, T., Miyoshi, H., Iwamura, H., and Anraku, Y. (1994) Identification of a novel quinone binding site in the cytochrome *bo* complex from *Escherichia coli*. Identification of a novel quinone-binding site in the cytochrome *bo* complex from *Escherichia coli*. *J. Biol. Chem.* **269**, 28908-28912
11. Sato-Watanabe, M., Itoh, S., Mogi, T., Matsuura, K., Miyoshi, H., and Anraku, Y. (1995) Stabilization of a semiquinone radical at the high affinity quinone binding site of the *Escherichia coli bo*-type ubiquinol oxidase. *FEBS Lett.* **374**, 265-269
12. Orii, Y., Mogi, T., Kawasaki, M., and Anraku, Y. (1994) Facilitated intramolecular electron transfer in the cytochrome *bo*-type ubiquinol oxidase initiated upon reaction of the fully-reduced enzyme with dioxygen. *FEBS Lett.* **352**, 151-154
13. Orii, Y., Mogi, T., Sato-Watanabe, M., Hirano, T., and Anraku, Y. (1995) Facilitated intramolecular electron transfer in the *Escherichia coli bo*-type ubiquinol oxidase requires chloride. *Biochemistry* **34**, 1127-1132
14. Woodruff, W.H. (1993) Coordination dynamics of heme-copper oxidases. The ligand shuttle and the control and coupling of electron transfer and proton translocation. *J. Bioenerg. Biomembr.* **25**, 177-188
15. Mogi, T., Hirano, T., Nakamura, H., Anraku, Y., and Orii, Y. (1995) CuB promotes both binding and reduction of dioxygen at the heme-copper binuclear center in the *Escherichia coli bo*-type ubiquinol oxidase. *FEBS Lett.* **370**, 259-263
16. Hirota, S., Mogi, T., Ogura, T., Hirano, T., Anraku, Y., and Kitagawa, T. (1994) Observation of the Fe-O_2 and Fe^{IV}=O Raman bands in dioxygen reduction by cytochrome *bo*-type ubiquinol oxidase from *Escherichia coli*. *FEBS Lett.* **352**, 67-70
17. Minagawa, J., Mogi, T., Gennis, R.B., and Anraku, Y. (1992) Identification of heme and copper ligands in subunit I of the cytochrome *bo* complex in *Escherichia coli*. *J. Biol. Chem.* **267**, 2096-2104
18. Uno, T., Mogi, T., Tsubaki, M., Nishimura, Y., and Anraku, Y. (1994) Resonance Raman and Fourier-transform infrared studies on the subunit I histidine mutants of the cytochrome *bo* complex in *Escherichia coli*: Molecular structure of redox centers. *J. Biol. Chem.* **269**, 11912-11920
19. Ingledew, J.W., Horrocks, J., and Salerno, J.C. (1993) Ligand binding to the haem-copper binuclear catalytic site of cytochrome *bo*, a respiratory quinol oxidase from *Escherichia coli*. *Eur. J. Biochem.* **212**, 657-664
20. Cheeseman, M.R., Watmough, N.J., Pires, C.A., Turner, R., Brittain, T., Gennis, R.B., Greenwood, C., and Thomson, A.J. (1993) Cytochrome *bo* from *Escherichia coli*: Identification of haem ligands and reaction of the reduced enzyme with carbon monoxide. *Biochem. J.* **289**, 709-718
21. Brudvig, G.W., Stevens, T.H., Morse, R.H., and Chan, S.I. (1981) Conformations of oxidized cytochrome *c* oxidase. *Biochemistry* **20**, 3912-3921
22. Cooper, C.E. and Salerno, J.C. (1992) Characterization of a novel $g'=2.95$ EPR signal from the binuclear center of mitochondrial

cytochrome *c* oxidase. *J. Biol. Chem.* **267**, 280-285
23. Calhoun, M. W., Gennis, R.B., Ingledew, W.J., and Salerno, J.C. (1994) Strong-field and integral spin-ligand complexes of the cytochrome *bo* quinol oxidase in *Escherichia coli* membrane preparations. *Biochim. Biophys. Acta* **1206**, 143-154
24. Watmough, N.J., Cheeseman, M.R., Gennis, R.B., Greenwood, C., and Thomson, A.J. (1993) Distinct form of the haem *o*-Cu binuclear center of oxidized cytochrome *bo* from *Escherichia coli*. Evidence from optical and EPR spectroscopy. *FEBS Lett.* **319**, 151-154
25. Tsubaki, M., Mogi, T., Hirota, S., Ogura, T., Kitagawa, T., and Anraku, Y. (1994) Molecular structure of redox metal centers of the cytochrome *bo* complex from *Escherichia coli*: Spectroscopic characterizations of the subunit I histidine mutant oxidases. *J. Biol. Chem.* **269**, 30861-30868
26. Hata, A., Kirino, Y., Matsuura, K., Itoh, S., Hiyama, T., Konishi, K., Kita, K., and Anraku, Y. (1985) Assignment of ESR signals of *Escherichia coli* terminal oxidase complexes. *Biochim. Biophys. Acta* **810**, 62-72
27. Watmough, N.J., Cheesman, M.R., Greenwood, C., and Thomson, A.J. (1994) Cytochrome *bo* from *Escherichia coli*: Reaction of the oxidized enzyme with hydrogen peroxide. *Biochem. J.* **300**, 469-475
28. Iwata, S., Ostermeier, C., Ludwig, B., and Michel, H. (1995) Structure at 2.8 Å resolution of cytochrome *c* oxidase from *Paracoccus denitrificans*. *Nature* **376**, 660-669
29. Tsukihara, T., Aoyama, H., Yamashita, E., Tomizaki, T., Yamaguchi, H., Shinzawa-Itoh, K., Nakashima, R., Yaono, R., and Yoshikawa, S. (1995) Structure of metal sites of oxidized bovine cytochrome *c* oxidase at 2.8 Å. *Science* **269**, 1069-1074
30. Thomas, J.W., Puustinen, A., Alben, J.O., Gennis, R.B., and Wikström, M. (1993) Substitution of asparagine for aspartate-135 in subunit I of the cytochrome *bo* ubiquinol oxidase of *Escherichia coli* eliminates proton-pumping activity. *Biochemistry* **32**, 10923-10928
31. Thomas, J.W., Lemieux, L.J., Alben, J.O., and Gennis, R.B. (1993) Site-directed mutagenesis of highly conserved residues in helix VIII of subunit I of the cytochrome *bo* ubiquinol oxidase from *Escherichia coli*: An amphipathic transmembrane helix that may be important in conveying proton. *Biochemistry* **32**, 11173-11180
32. Kita, K., Konishi, K., and Anraku, Y. (1984) Terminal oxidases of *Escherichia coli* aerobic respiratory chain. I. Purification and properties of cytochrome b_{562}-*o* complex from cells in the early exponential phase of aerobic growth. *J. Biol. Chem.* **259**, 3368-3374
33. Moody, A.J., Rumbley, J.N., Gennis, R.B., Ingledew, W.J., and Rich, P.R. (1993) Ligand-binding properties and heterogeneity of cytochrome *bo* from *Escherichia coli*. *Biochim. Biophys. Acta* **1141**, 321-329
34. Tsukihara, T., Aoyama, H., Yamashita, E., Tomizaki, T., Yamaguchi, H., Shinzawa-Itoh, K., Nakashima, R., Yaono, R., and Yoshikawa, S. (1996) The whole structure of the 13-subunit oxidized cytochrome *c* oxidase at 2.8 Å. *Science* **272**, 1136-1144
35. Puustinen, A., Verkhovsky, M.I., Morgan, J.E., Belevich, N.P., and Wikström, M. (1996) Reaction of the *Escherichia coli* quinol oxidase cytochrome bo_3 with dioxygen: The role of a bound ubiquinone molecule. *Proc. Natl. Acad. Sci. USA* **93**, 1545-1548
36. Geier, B.M., Schägger, H., Ortwein, C., Link, T.A., Haggen, W.R., Brandt, U., and von Jagow, G. (1995) Kinetic properties and ligand binding of the eleven-subunit cytochrome-*c* oxidase from *Saccharomyces cerevisiae* isolated with a novel large-scale purification method. *Eur. J. Biochem.* **227**, 296-302
37. Moody, A.J., Cooper, C.E., and Rich, P.R. (1991) Characterization of 'fast' and 'slow' forms of bovine heart cytochrome-*c* oxidase. *Biochim. Biophys. Acta* **1059**, 189-207
38. van Gelder, B.F. and Beinert, H. (1969) Studies of the heme components of cytochrome *c* oxidase by EPR spectroscopy. *Biochim. Biophys. Acta* **189**, 1-24
39. Ingredew, W.J. and Bacon, M. (1990) A comparative review of the structure and function of cytochrome *o* from *Escherichia coli* and cytochrome aa_3. *Biochem. Soc. Trans.* **19**, 613-616
40. Powers, L.S., Lauraeus, M., Reddy, K.S., Chance, B., and Wikström, M. (1994) Structure of the binuclear heme iron-copper site in the quinol-oxidizing cytochrome aa_3 from *Bacillus subtilis*. *Biochim. Biophys. Acta* **1183**, 504-512
41. Powers, L., Chance, B., Ching, Y., and Angiolillo, P. (1981) Structural features and the reaction mechanism of cytochrome oxidase. Iron and copper X-ray absorption fine structure. *Biophys. J.* **34**, 465-498
42. Wang, Z., Asenjo, A.B., and Oprian, D.D. (1993) Identification of the chloride-binding site in the human red and green color vision pigments. *Biochemistry* **32**, 2125-2130
43. Schultz, S.G., Wilson, N.L., and Epstein, W. (1962) Cation transport in *Escherichia coli*. II. Intracellular chloride concentration. *J. Gen. Physiol.* **46**, 159-166